High landscape-scale forest cover favours cold-adapted plant communities in agriculture–forest mosaics

Jeremy Borderieux, Jean-claude Gégout, Josep Serra-Diaz

This manuscript was published in *Global Ecology and Biogeography* in March 2023
DOI: https://doi.org/10.1111/geb.13676

High landscape-scale forest cover favors cold-adapted plant communities in agriculture-forest mosaics

Jeremy Borderieux[1, *], Jean-Claude Gégout[1], Josep M. Serra-Diaz[1 2]

Corresponding author: Jeremy Borderieux: jeremy.borderieux@agroparistech.fr

1. Université de Lorraine, AgroParisTech, INRAE, UMR Silva, 54000 Nancy, France

2. Eversource Energy Center and Department of Ecology and Evolutionary Biology, University of Connecticut, Storrs, CT, United States of America

Abstract

Aim: The ongoing climate warming is expected to reshuffle understory plant-community composition by increasing the occurrence of warm-adapted species at the expense of cold-adapted species. Previous studies have evidenced a warming Community Temperature Index (CTI) over time. However, data indicate that the local tree canopy can partly explain an observed lag between understory plant CTI and climate warming rates, though landscape-scale forest cover effects have not yet been investigated. Here, we test the hypothesis that the amount of forest cover in the landscape lowers local CTI.

Location: Temperate forests in France.

Time period: 2005 - 2019

Major taxa studied: Forest vascular plants.

Methods: We compared 2,012 pairs of neighboring French forest inventory plots with contrasting percentages of forest cover within a 1-km radius area (landscape forest cover). We computed the difference in the CTI of the understory communities for each pair and tested the contribution of the landscape-scale forest cover, local canopy cover, and soil conditions to the differences in CTI.

Results: Plots located in highly forested areas (>80% in the 1km area) had an average CTI 0.26 °C lower (0.81°C s.d.) than plots in sparsely forested areas (<30% in a 1km area). Fifty percent of this difference was explained by landscape-scale forest cover. Bioindicated soil conditions such as pH and available nutrients, which correlated with cold-adapted species preferences, explained the remaining 50%.

Main conclusions: Highly forested landscapes allow colder-adapted species to survive in given macroclimatic conditions. These landscapes meet cold-adapted species soil requirements and may cool the regional climate. Further microclimatic studies are needed to confirm the cooling capacity of landscape-scale forest cover.

Keywords

plant community, landscape ecology, forest fragmentation, global warming, forest inventory, mesoclimate, microclimate

1. Introduction

Climate change and land-use change are the main drivers of past and current plant diversity. These drivers and their interaction are leading to shifts in species distribution, the extinction of the most vulnerable species, and a reshuffling of existing communities (Franklin et al., 2016; Kuhn & Gégout, 2019; Pecl et al., 2017; Thomas et al., 2004). The flora of the forest understory makes up 80% of forest vascular plant diversity and plays a key role in many ecosystem functions (Landuyt et al., 2019). Likewise, understory flora is being increasingly considered in forest management decisions in the face of climate change (Blondeel et al., 2021; Gilliam, 2007; Landuyt et al., 2019), and in global forest conservation and restoration efforts (Stanturf et al., 2014).

The influence of free-air temperature (the macroclimate) on understory communities is buffered by the cover of local overstory trees (De Lombaerde et al., 2021; Godefroid et al., 2006; Maclean et al., 2015; Zellweger et al., 2020). Tree cover in temperate forests creates an understory microclimate characterized by cooler maximum temperatures and warmer minimum temperatures. Microclimate depends on local stand conditions, but is also driven by broader scale factors. Topography for example is an important factor that can influence temperature through elevation, aspect, cold air pooling, as is macroclimate, which is determined by drivers such as latitude, solar radiation and distance to the coast. The effect of local tree cover on the understory microclimate and species communities is increasingly under study; however, less is known about the effect of landscape-scale forest cover on understory composition.

The forest habitats in central European landscapes have typically undergone intensive logging in the past, which has resulted in the current mosaic of forest patches of different sizes. These patches, where forest understory species may persist under existing tree cover, are embedded in an extensive agricultural matrix (IES, 2013). The influence of landscape-scale forest cover on the regional climate is still under debate and is currently the subject of many studies, since forest cover at the landscape scale involves two processes pulling in opposite directions. On the one hand, temperatures may increase with increasing forest cover because a forest's albedo is lower than other land cover types like grasslands and croplands. This warming effect is most apparent in cooler seasons, when forests do not retain the snow cover and release a latent heat flux at night. On the other hand, forests have a cooling influence during warmer seasons, stemming from their higher evapotranspiration, which directly cools the air and promotes cloud formation (Bonan, 2008;

Hesslerová et al., 2013; Pokorny et al., 2010). The growing season is a critical period for both annual and perennial cold-adapted species. One could therefore expect that landscape-scale forest cover could benefit plant species by cooling the hotter and drier (mean and extreme) conditions in spring and summer that could induce the dieback of vulnerable species. In those landscapes, the community could also be comprised of cold-adapted species because they can outcompete the warmer-adapted species located at their cold edge of their distribution (Sanczuk et al., 2022). Highly forested landscapes could also influence plant-community composition and favor cold-adapted species through other means. For example, large forest patches in central Europe historically grow on low-nutrient soils unsuitable for agriculture, and are less influenced by fertilization from nearby croplands than small forest patches (Bergès et al., 2016). This is relevant as the cold-adapted species in Europe are also adapted to poorer soil conditions (Ewald, 2003). Taken together, these two characteristics increase the potential for highly forested landscapes to conserve cold-adapted species.

In this study, we investigated the role of forest cover in the surrounding landscape on plot-scale (i.e. local) plant-community composition in agricultural-forest mosaics in the temperate biome. We carried out pairwise comparisons of forest plots with contrasted landscape-scale forest cover (1km area), and used community temperature index (CTI) as a proxy for community adaptation to climate. CTI is calculated as the average thermal optimum of the recorded species of a plot. The thermal optimum of a species is estimated from a species maximum probability of occurrence along the temperature gradient and therefore reflects the climate that the species experiences in its biogeographic area. CTI may be used to compare a species' or a community's tolerance to the warming climate; a large difference between the current climate and a species' optimum can be an early warning sign of local or regional extinctions (Kuhn & Gégout, 2019).

We hypothesized that (1) plant communities surrounded by highly forested areas would have a lower CTI than those located in landscapes with little forest cover; that (2) there would be a pure landscape-forest cover effect, which, (3) together with soil factors, would explain the differences in CTI.

2. Materials and methods

a. Overview

We used floristic surveys from the French National Forest Inventory (NFI) and a 20-meter resolution forest cover map to test the influence of forest cover in the surroundings on local

Community Temperature Index (CTI). This CTI aggregated the thermal optima of every species on a given plot, thus reflecting the mean climatic preference of the community. We used pairwise comparisons to reveal differences in the CTI (ΔCTI) of geographically close plots (<5 km from each other) with contrasting landscape-scale forest cover (high vs. low forest cover, calculated within a 1-km-radius area) in a French temperate lowland forest. We then used a linear model to analyze the effect of bioindicated soil conditions, local canopy cover, distance to the forest edge, and difference in landscape-scale forest cover on ΔCTI. We tested the robustness and the relationship between ΔCTI and landscape-scale forest cover by repeating the analysis at different landscape-forest-cover thresholds to separate high vs. low landscape-scale forest cover.

b. Floristic surveys and landscape-scale forest cover.

We extracted plant-community data from the French National Forest Inventory (NFI). NFI surveys are based on a 1km-by-1km grid sampling scheme. One tenth of the grid nodes (equally-distanced plots) are surveyed each year to ensure spatial and temporal representativeness for French forests. We extracted our study plots from the NFI surveys from 2005 to 2019.

Each NFI plot has a circular nested design where different variables are measured at varying radii from the plot center. The floristic surveys used in our study were performed within a 15-meter-radius circle (area = 709 m^2).The taxonomy of the described flora was standardized to the *Euro+ Med PlantBase* taxonomy (Euro + Med, 2006). We removed tree species and the other main woody species from our data, since the presence of trees in the understory is sensitive to management, and because woody species respond more slowly to environmental factors than do herbaceous forest species. We also removed species that had not been identified to the species level.

NFI canopy cover data is estimated at the plot level through visual observation of the light intercepted by the canopy within a 25-meter-radius circle; cover cannot exceed 100%. We extracted the mean annual temperature (hereafter MAT) for each plot from a model calibrated with 214 French weather stations (Piedallu et al., 2019). We extracted elevation from a 25m-resolution digital elevation model produced by the National Geographic Institute (BD_topo).

We obtained the landscape-scale forest cover for each plot by computing the percentage of forest cover in the surrounding 1km-radius area. We selected a 1km radius to capture the immediate surroundings of the plots and to compensate for the fuzziness (± 250 m) of the coordinates the NFI provides to protect private property. This 1km radius is coherent with remote sensing studies that have shown an effect of forest cover on regional climate at a 5km-by-5km scale (Li et al., 2015; Prevedello et al., 2019). Forest cover data were obtained

from ‘BD_Foret V2’, a 20m-resolution forest map (IGN, 2019). This map was produced through photo interpretation of infrared images and adheres to the definition of a forest established by the Food and Agriculture Organization (FAO), i.e. a surface area exceeding 0.5 ha with more than 10 % tree cover. Lastly, we used the boundaries of the BD_Foret V2 map to compute the distance to the nearest forest edge for a few plots, for which the true coordinates were available (the 2006 to 2011campaign).

c. Calculating Community Temperature Index and soil conditions bioindication

We calculated CTI as the mean of the thermal optima of all the non-tree vascular plant species occurring in the plot. The species’ thermal optima were extracted from the ClimPlant database (Vangansbeke et al., 2021). This database provides thermal optimum estimates based on distribution atlases and the 10km-resolution 1971-2000 climate data of WorldClim v2 (Fick & Hijmans, 2017) at the European scale. The database covers the entire distribution of the species we recorded, thus providing us with an accurate estimation of their thermal optima. For the 844 different species recorded, we obtained 508 species’ thermal optima. On average, a plot hosted 13 (s.d. 7.4) species with a known thermal optimum, representing 78% (s.d. 13%) of the studied species of a plot. Species with no thermal optimum were mostly rare or endemic species.

To go beyond climate, we also selected soil pH and nutrient availability as possible explanatory variables for, differences in CTI between plots with high and low landscape forest cover. This step was critical since evolutionary adaptation may create a correlation between climate and soil preferences for plant species. For instance, cold-adapted species are generally also adapted to acidic soils (Ewald, 2003; Szymura et al., 2014). The litter in cold forests is more likely to have slow biotic activity (low temperature, low nutrients conifer needles), which reduces nutrient cycling and availability (Osman, 2013). By including soil information, we were also to able to isolate the contribution of climate factors to CTI.

We extracted species pH indicator values from the EcoPlant database (Gégout et al., 2005), a phytosociological database linking floristic surveys and soil analyses. We extracted species nitrogen and light requirements, respectively Ellenberg N and L, from Ellenberg et al. (1992), a large survey of expert knowledge on plant ecology. We assigned a pH indicator value and an Ellenberg N and L value to respectively 512, 429 and 453 species, encompassing 92%, 61% and 69% of the total occurrences in our dataset. We then calculated the bioindicated (inferred from the flora) pH, nitrogen availability and light at each plot by averaging the indicator values of the species present without weighting by abundance (Carpenter & Goodenough, 2014). To improve the reliability of our soil bioindication, we

maximized the number of species used in our calculations by including all the species possible, even those without a thermal optimum value.

d. Study area, plot selection, and geographical pairing of the plots

Our study site was located in the French temperate broadleaf and mixed-forest biome where 31% of the land cover is forested (IGN, 2019). The climate is oceanic to continental (with larger temperature amplitudes) and the MAT ranges from 8 to 11°C (Météo France weather stations; Piedallu et al., 2019). The study area included mountain ranges, but the strict selection procedure described hereafter mainly focused on lowland areas characterized by alternating expanses of croplands, grazing land and deciduous forest patches of different sizes.

We selected NFI plots exclusive to this biome, and refined our selection with two criteria: (1) the plots had to be forested – as opposed to open land or recent clear-cuts, and (2) to ensure the quality of the CTI value, the plots had to host more than five species for which thermal optimum information was available.

The plots with more than 80% of forested area within a 1km radius (251 ha) were classified as "forested" (F) and those with less than 30% (94 ha) were classified as "non-forested" (NF). We selected pairs of "forested" vs. "non-forested" plots based on two constraints: (1) the distance between the plots was <5 km, and (2) the elevation difference was <50 m. These criteria allowed us to minimize the macroclimatic differences between plots. In order to give the same weight to each plot, a given plot was only included in one pair. We used an algorithm to maximize the number of possible pairs respecting the two constraints: we first paired isolated plots, then paired the plots with many neighbors (see the Data Availability section for codes). This process resulted in a larger sample size of paired plots, although the mean distance between the plots of a pair was not minimized.

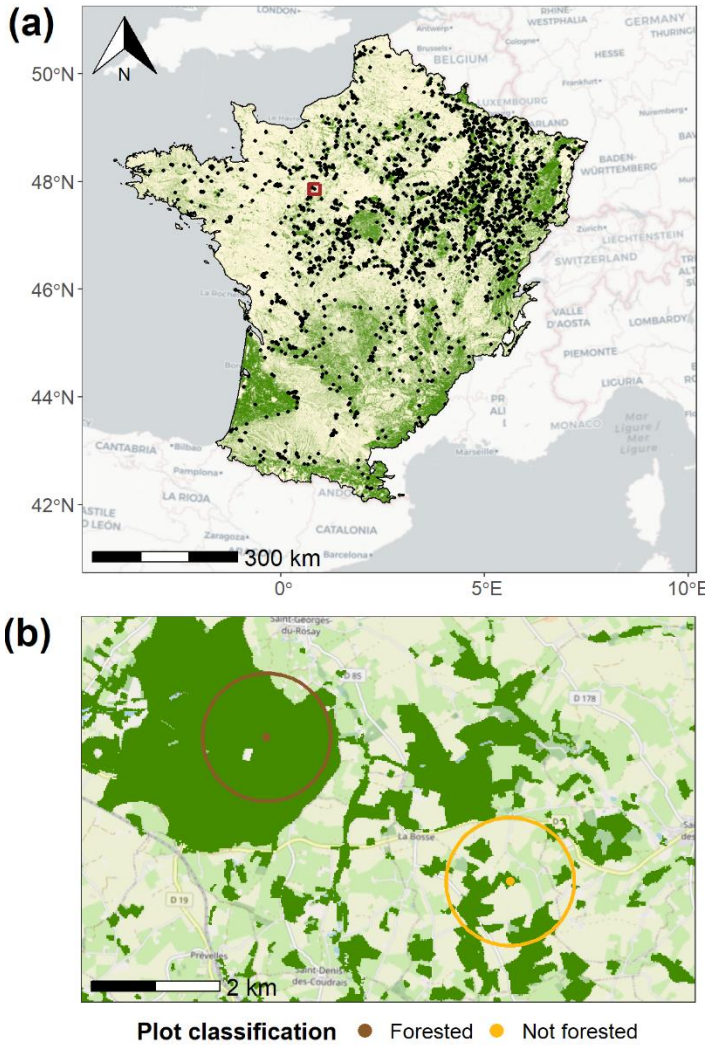

Figure 1: (a) Map of the study area, dots are the centroids of each National Forest Inventory plot pair, background map is a 1km resolution forest cover map of France (IGN, 2019)*, brown inset indicates the location of the (b) map.*

(b) Close-up map of a plot pair, dots are the NFI plots, circles are the surrounding area used to compute the percentage of forest cover in the landscape, and dark green is the forest cover at a 20m resolution. Basemaps credits: OpenStreetMap

The final dataset contained 4,024 plots arranged into 2,012 pairs (Fig. 1.a). The mean distance between two plots in a pair was 3.6 km (see Fig. 1.b for an example). The maximum and minimum distances between plots were 5km and 1km (NFI grid resolution), respectively. F and NF plots were similar in terms of macroclimatic mean annual air temperature, with a mean average difference of only 0.06 C° across all plots (Table 1). The plot-scale basal area and canopy cover differed by 2.1 m^2/ha and 0.6%, respectively (Table 1). Average pH and mean Ellenberg N values differed between the two landscape classes: they were higher in NF than in F plots by 0.8 and 0.9, respectively (Table 1).

Table 1: Environmental characteristics of Forest (F) versus non-forest (NF) plots. Mean of environmental, landscape and stand variables per plot classification (5^{th} and 95^{th} quantiles in parentheses). Landscape forest cover is estimated within a 1km radius around the plot.

Landscape Of The Plot	Number Of Plots	Mean Annual Temperature (°C)	Elevation (M)	Landscape Forest Cover (Ha)	Landscape Forest Cover (%)	Mean Ellenberg N	Bioindicated Ph	Basal Area (M^2/Ha)	Canopy Cover (%)
Non-forested (NF)	2012	11.00 (9.68-12.91)	252 (61-633)	62 (19-92)	19.9 (6.2-29.2)	5.3 (3.4-6.7)	6.2 (4.6-7.2)	24.7 (4.6-49.7)	78.3 (30-100)
Forested (F)	2012	10.94 (9.69-12.81)	262 (71-639)	281 (254-312)	89.4 (80.8-99.4)	4.4 (2.7-5.9)	5.4 (4-6.8)	22.8 (5.2-42.6)	78.9 (30-100)

e. Statistical analyses

We used a Wilcoxon ranked test to test whether the difference in CTI (hereafter ΔCTI) between the F and the NF plots was significantly different from 0.

To test whether variables other than the difference in landscape-scale forest cover (F vs NF) could explain ΔCTI, we used a linear model with ΔCTI as the dependent variable, and the pairwise differences of the other candidate factors as independent variables. The variables tested were bioindicated pH, mean Ellenberg N and L indices, year of survey, elevation and MAT. A stepwise AIC (Akaike Information Criterion) procedure determined the final model when the addition or the deletion of a variable did not reduce the AIC by more than 2 points (Akaike, 1974).

We also tested for canopy cover and distance to the forest edge, two determinants of understory microclimate (Meeussen et al., 2021; Zellweger et al., 2020). Canopy cover values were only available for 1,940 pairs, and distance to the forest edge for 309 pairs. Consequently, we ran the variable selection procedure on the complete dataset (2,012 pairs) without these two variables. We then fitted the selected model with the addition of the canopy cover or the distance to the edge variable to the appropriate subset of the complete dataset. We thus obtained three models: the model for the complete dataset, the canopy cover model, and the distance-to-forest-edge model.

The model formulation is summarized in equation (*1*),

$$\Delta CTI = intercept + \beta_i * \Delta_i + \varepsilon \quad (1)$$

where ΔCTI is the CTI of the F plot minus the CTI of the NF plot for each plot pair; Δ_i is the subtraction of an explanatory variable i for the same F-NF pair, and ε is the error term of mean 0, following a normal distribution. β_i is the fitted parameter testing the effect of Δ_i. Any significant difference of a parameter from 0 was assessed with a Wald test. The interest of this formulation is that all the covariables (Δ_i) are differences. If these covariables are

set to 0, the intercept represents the effect of a difference in landscape forest cover (F vs NF) *per se*, all other environmental variables considered.

To quantify the effect the predictors had on ΔCTI, we computed effect size by multiplying the fitted parameter β_i by the mean of Δ_i. For example, a difference Δ_i can be strongly correlated with ΔCTI at the pair level, but have no effect on overall ΔCTI because Δ_i is close to 0.

We checked for residual normality, absence of collinearity among the predictors, homoscedasticity and independence from the other variables not included in the models (Zuur et al., 2010). The above requirements were met for all of the models tested.

We further assessed the robustness of our results by testing different thresholds to separate the F vs. NF classes. Specifically, we ran the above-mentioned analysis (2.d, 2.e) with a varying threshold for F plots. This threshold ranged from [30% – 50%] of forest cover in the 1km radius to [80% - 100%] by increments of 5%. The NF plot classification was kept constant [0% - 30%]. This resulted in a total of eleven assessments of landscape-scale forest effects.

All analyses were performed with the R software v 3.6.1 (R Core Team, 2019) and the 'sf' (Pebesma, 2018), 'raster' (Hijmans, 2020) 'data.table' (Dowle & Srinivasan, 2020), 'ggplot2' (Wickham, 2011) and 'ggspatial' (Dunnington & Thorne, 2020) packages.

3. Results

The plots in forested landscapes (F) had an average CTI 0.26°C lower than the plots in non-forested landscapes (NF) ($P<0.001$). The difference in CTI between F and NF plots was highly variable (0.81°C s.d.). In 63% of the plot pairs, F plots had a lower CTI (the difference was negative), and for 17% of the pairs this difference was more than -1°C (Fig. 2). Conversely, for 37% of the plot pairs, the F plots had a higher CTI, and the difference was more than +1C° for 6% of the pairs. Differences in CTI ranged from -3.5°C to +3.0°C (Fig. 2).

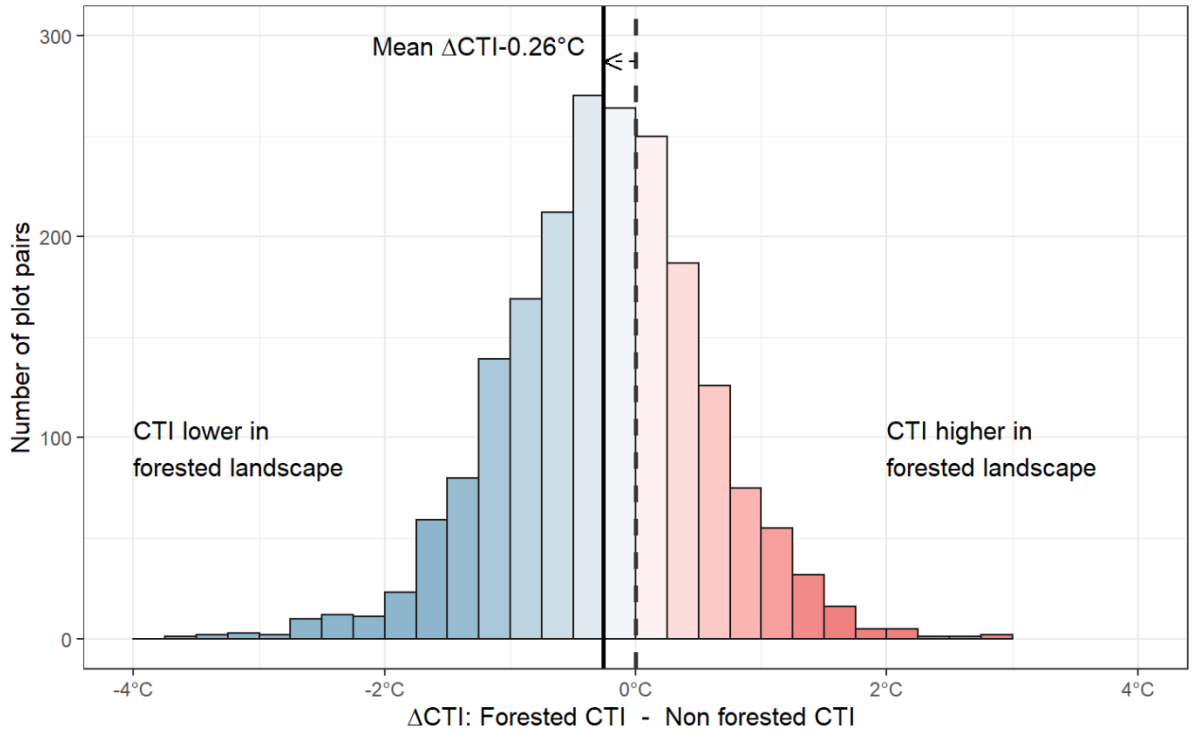

Figure 2: Distribution of the difference in Community Temperature Index (CTI, °C) for all plot pairwise differences (n= 2,012). A negative difference means that the forested plot in the pair displayed a cooler CTI. The solid vertical line represents the mean of this difference, the dashed vertical line indicates no pairwise difference (0 °C).

We found only minor effects, that is significant but negligible effects, (effect size < 0.03°C) for ΔElevation, ΔMAT, ΔEllenberg L and ΔYear on pairwise differences in CTI (Table 2). However, the effects of ΔBioindicated pH and ΔEllenberg N had more importance on ΔCTI: -0.24°C and 0.11°C, respectively (Table 2). This greater effect size was caused by the important difference between the F and NF plots for the two soil parameters (Table 1). In our subset of species, thermal optimum was positively correlated, with low statistical significance, with the pH indicator value (coefficient: 0.16, P<0.10, Fig. S1, Table S3). Thermal optima and N Ellenberg values were not correlated (P=0.40, Table S3).

Table 2: Linear model results relating differences in Community Temperature Index (CTI) to different drivers. Coefficients (Estimate), Standard errors, P-values, effect size of the parameter, and adjusted R^2 for the linear model predicting the pairwise difference in CTI. Effect sizes were computed by multiplying an estimate by the mean pairwise difference of the corresponding parameter (except for the intercept).

Parameters	Estimate	Std. Error	P-value	Effect size	R^2
Intercept	-0.133	0.024	$<10^{-4}$	-0.13	0.122
ΔElevation	0.00274	0.00082	$<10^{-4}$	0.027	
ΔMAT	0.279	0.086	0.0013	-0.016	
ΔEllenberg L	-0.199	0.019	$<10^{-4}$	0.0074	

ΔBIOINDICATED PH	0.318	0.025	$<10^{-4}$	-0.24
ΔELLENBERG N	-0.131	0.02	$<10^{-4}$	0.11
ΔYEAR	0.00639	0.0031	0.038	-0.0093

We found a significant effect of local canopy cover on ΔCTI. This effect however contributed marginally (effect size=0.001°C) to lower CTI in F plots because F and NF plots had on average the same local canopy cover (Table 1, Table S1). We found no significant effect of distance to forest edge on ΔCTI (P=0.42, Table S2). It should be noted that these two results do not imply that canopy cover or distance to forest edge are unrelated to CTI. Rather, they showed that the balance of those variables created by the pairwise selection successfully reduced their effect size to be negligible.

We fitted our linear model with only pairwise differences as a predictor. As a result, setting the differences to 0 meant that the model compared the F and NF categories with all other factors considered to be equal. Thus, the significant intercept we found indicated a decreased in CTI in F plots not explained by any other factors than the difference in landscape classification (NF vs F, Table 2). The lower CTI in the F plots was robust to different F-NF classification thresholds (e.g. highly forested landscapes, Fig. 3) but lower CTIs were especially apparent in landscapes with >70% total forest cover. Effect sizes of the other factors playing a significant role were also robust to changes in NF-F classification thresholds. The decrease in ΔCTI and the contribution of the other factors to it were linear, we did not detect a saturation effect of increasing landscape-scale cover effect.

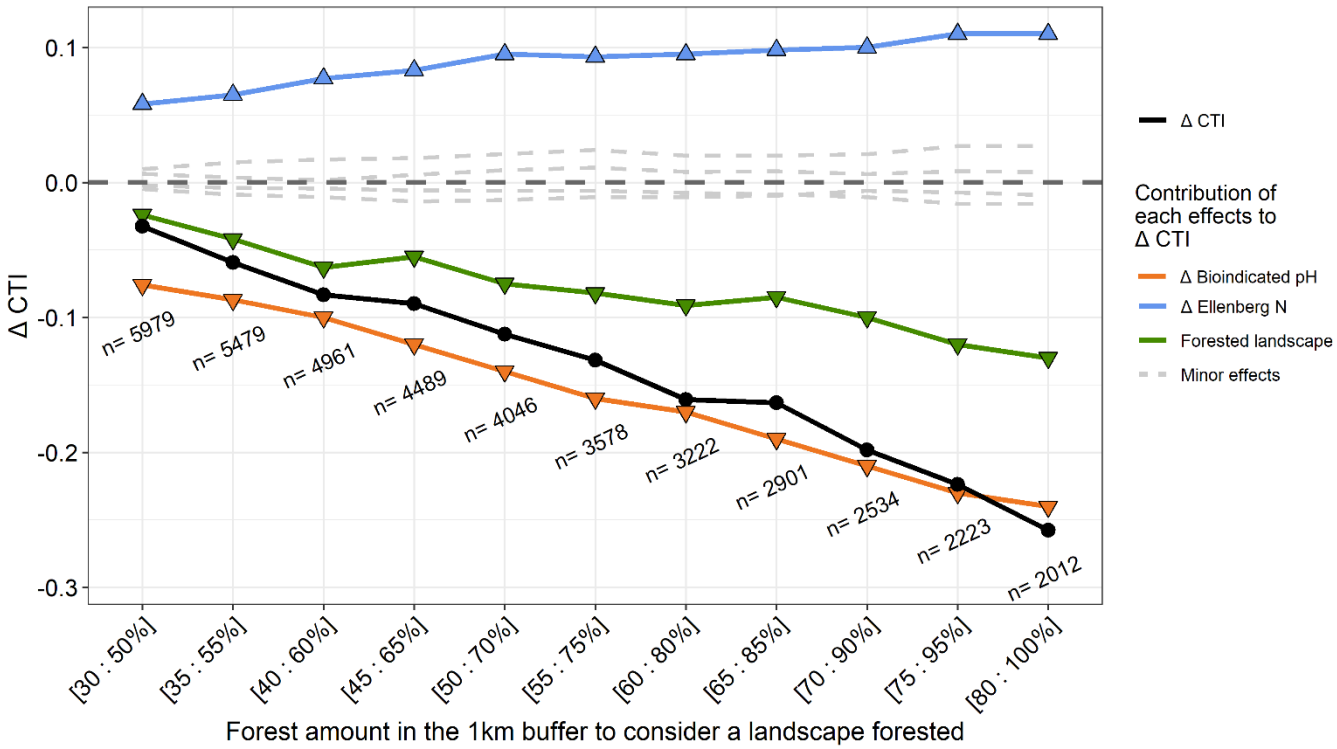

Figure 3: Difference in CTI between a "forested" and a "non-forested" plot (black line) as a function of how much total forest cover surrounds a "forested" plot. A negative value means that the forested plot has a cooler community. Colored lines are the contribution (effect sizes) of the most important drivers of this difference. Effect sizes were computed by multiplying the fitted parameter of a driver to the mean of its difference between "forested" and "non-forested" plots. The number of plot pairs for each analysis is shown. Minor effects are significant predictors but with negligible effect size. Minor effects are: year of the survey, elevation, mean annual temperature and Mean Ellenberg L.

4. Discussion

Our results indicate that the CTI of vascular plants in forest understories is 0.26°C lower in forested landscapes than in unforested landscapes. This result can be compared with the recent community thermophilization rates (increasing CTI over time) of ca. 0.1°C per decade found in temperate forest plant communities (Dietz et al., 2020; Martin et al., 2019; Richard et al., 2021), and with recent air-temperature warming rates of ca. 0.26 °C per decade (2002 to 2018) in our study area (Dietz et al., 2020). We found a significant spatial pattern for the CTI of forest understory plants equivalent to three decades of thermophilization, or one decade of macroclimatic warming. By controlling for canopy cover and distance to forest edge, we show that the lower CTI in highly forested landscapes is explained by differences in soil conditions (pH and nutrient content) that favor cold-adapted species. The structure of our sampling allowed us to observe a landscape-scale forest cover cooling on CTI *per se*.

In our study, bioindicated soil characteristics (Ph and nutrient content) drove 50% of the difference in CTI between F and NF plots (0.13°C). In landscapes with less than 30% forest cover, the understory plant communities in our plots were characterized by species requiring nutrient-rich soils and high pH, and by nitrophilous species. These species had higher thermal optima, thus creating a significant (albeit weak) correlation between soil and climate preference (Fig. S1, Table S3). On average, soil pH and mean N Ellenberg values were respectively 0.8 and 0.9 lower in F plots (Table 1). These differences may have affected the CTI, as an increase of 1 in a pH indicator value increases the thermal optimum of a species by 0.16 C° (Table S3). Correlations of thermal optimum and soil preferences have been documented before (Ewald, 2003), they may results from adaptation of to poor soils found of cold forests (Osman, 2013).

Landscape forest cover was therefore linked to local soil conditions we observed in the F and NF classes (Table 1). In addition, pH and nitrogen are both very sensitive to past agricultural practices. Small forests are more likely to be younger forests growing on past agricultural lands in our study region, as shown by historical maps made in cir. 1750 (Vallauri

et al., 2012). The smaller (and generally younger) forests display high nutrient loads because they are located on former agricultural lands, and conversely, the larger forests historically grow on less fertile soils (Bergès et al., 2016). Furthermore, smaller forest patches and forest edges are more affected by horizontal fertilization from nearby fields, and by atmospheric N deposition (Bergès et al., 2016). Agricultural mosaics make up most European forests' immediate surroundings (IES., 2013). Our findings could therefore be applied in most temperate European forests, where the species pool and agriculture mosaics are similar .

The remaining effect of 0.13°C at the intercept of the model represents an effect that none of the other included variables explained, and which can be attributed to the difference in landscape forest cover. The lower CTI in the forested landscapes implies that the species therein have biogeographic origin of cooler climate. Such species can be present due to legacy effects; cold-adapted species are associated with old-growth forests (Bodin et al., 2013; Dupouey et al., 2002; Ewald, 2003). The remnants of old growth forests in France tend to be large forests that fall into our definition of forested landscapes (Vallauri et al., 2012). Cold-adapted forest species also have limited dispersal capacity (Dupouey et al., 2002). The larger forests in the landscapes with high forest cover could favor species with low dispersal capacity since connectivity is increased in large, closely-knit forest habitats (Saura et al., 2014). We cannot exclude the possibility that parts of our results originate from the temporal dynamic of CTI, that is, thermophilization, as our study is set in a fixed time span and could be a snapshot of different thermophilization rates (Richard et al., 2021).
In our analyses, we controlled for microclimatic effects. We carried out balanced plot pairing and added two well documented determinants of forest microclimate - immediate canopy cover and distance to forest edge - to our sub-models (Chen et al., 1999; De Frenne et al., 2019; Meeussen et al., 2021). The effect of the landscape-scale forest cover remained significant with these controls. This indicates that landscape-scale forest cover may have a cooling effect on regional temperatures, with a subsequent effect on the understory. Forests have higher evapotranspiration than other land cover types such as cropland and grasslands, thereby lowering the air temperature and promoting cloud formation. The forest cover can cool the regional climate during the growing season (Bonan, 2008; Hesslerová et al., 2013; Pokorny et al., 2010), and this service is critical for the survival of understory plants , especially cold-adapted species, during the hot summer months. Indeed, the conditions in the understory depend on local stand structure, but also on the regional climate (De Frenne et al., 2021).

Our results show a large variability in CTI differences between the F and NF plots (Fig. 1). Indeed, 37% of the F plots had a higher CTI than the NF plots. This is most likely due to sampling conditions. CTI is sensitive to changes in community composition when the number of occurrences is low. Furthermore, though we selected geographically close plots with contrasting landscape-scale forest cover to balance the environmental and stand variables of the two large classes F and NF for the whole dataset (Table 1), some individual pairs no doubt differed in stand conditions (e.g. canopy cover). Such conditions influence the microclimate (De Frenne et al., 2013) and this contributed to the large variability in differences we found in the full sample. Finally, we do not exclude the possible impact of other landscape such as water bodies, urbanized areas, complex edge structures or topographic elements that could significantly influence climate and community dynamics (Meeussen et al., 2021).

Our study relied on plant species indicator values but their use is controversial since indicators can be poorly correlated with actual measurements as they are sometimes derived from expert knowledge (Marrec et al., 2022; Szymura et al., 2014). We strengthened our analysis by including the pH indicator value from Gégout et al., (2005), which was calibrated with soil measurements and a floristic survey database. We maintain that it was useful to include these indicator variables in our study as a proxy for excess fertilization from nearby previous and current agricultural activities. Similarly, we combined Ellenberg L (light) values, when available, and canopy cover data (in one of the sub-model) to better account for canopy density and light conditions.
We used the mean of the recorded understory thermal optima as our response variable. The thermal optima in ClimPlant were computed from distribution maps and grids of macroclimatic temperature (Vangansbeke et al., 2021). These indices are valuable to infer the biogeographic origin of a species. We interpreted cooler CTI within a highly forested landscapes as a regional cooling favoring those species. However, the potential of CTI to infer direct microclimatic temperature is limited (Marrec et al., 2022), future research including microclimatic measurements or analysis of readily available weather station data, will be critical to further elucidating the climatic versus soil effects contributing to the persistence of cold-adapted species observed in our study.

Current climate warming is likely to have particularly harmful effects on cold-adapted species, which may escape regional warming by retracting to climate refugia with locally cooler and more suitable microclimates(Corlett & Westcott, 2013; Hylander et al., 2022; Kuhn & Gégout, 2019). For forest species, these climatic refugia can be topographic (e.g.

cold air pooling) (Stark & Fridley, 2022), dense forests (Frey et al., 2016) or even hedgerows in open landscapes (Vanneste et al., 2020). Our study highlights that highly forested landscapes also promote the presence of cold-adapted species, a refugia that is expected to last as the buffering capacity of forest will stay constant or increase with climate change (De Lombaerde et al., 2021). Our results however should not be used to undermine the importance of small forest patches in agriculture mosaics (Valdés et al., 2020). Forests in landscapes with limited forest cover harbor on average warm-adapted species, which are more suited to the warmer climate and are more resilient in the face of disturbances. that could rapidly remove the forest buffering capacity (Christiansen et al., 2021; Hylander et al., 2022). In addition, our results (Fig. 3) show a linear decrease, without saturation, in CTI with increasing landscape-scale forest cover, as a result, any amount of forest cover in the landscape can have an effect on CTI. This implies that landscape-scale forest cover diversity also matters for understory plant diversity by providing a set of different soil and thermal conditions for a variety of species. Acknowledging such heterogeneity and the potential refugia of large forests is one of the keys to successful forest biodiversity conservation at the landscape scale (Hylander et al., 2022). We acknowledge that part of the difference in CTI could be driven by the colonization of warm-adapted generalist species in edges and low forested landscapes. We chose to emphasize the presence of cold-adapted species in "forested" plots as they are the most threatened by climate change, and are most discussed in recent conservation literature (Hylander et al., 2022). In addition, our regional cooling interpretation complement the current literature on the potential protection forest microclimate offers in the warm edge of the distribution of cold-adapted species (De Frenne et al., 2021; Sanczuk et al., 2022).

Current land use changes will likely drive changes in forest cover and forest distribution (Doelman et al., 2018; Ellis, 2021). We demonstrate that the mean thermal optimum of an understory plant community is sensitive to the amount of forest around it. Large forest masses harbor on average more cold-adapted species, and landscapes with forest patches of contrasting sizes may provide a suite of opportunities for different species. As the climate continues to warm, guaranteeing the availability of both forested and diverse landscapes will be key to ensuring biodiversity protection and ecosystem adaptation and resilience in the near and distant future.

5. References

Akaike, H. (1974). A new look at the statistical model identification. *IEEE Transactions on Automatic Control*, *19*(6), 716–723. https://doi.org/10.1109/TAC.1974.1100705

Bergès, L., Avon, C., Arnaudet, L., Archaux, F., Chauchard, S., & Dupouey, J.-L. (2016). Past landscape explains forest periphery-to-core gradient of understorey plant communities in a reforestation context. *Diversity and Distributions*, *22*(1), 3–16. https://doi.org/10.1111/ddi.12384

Blondeel, H., Landuyt, D., Vangansbeke, P., De Frenne, P., Verheyen, K., & Perring, M. P. (2021). The need for an understory decision support system for temperate deciduous forest management. *Forest Ecology and Management*, *480*, 118634. https://doi.org/10.1016/j.foreco.2020.118634

Bodin, J., Badeau, V., Bruno, E., Cluzeau, C., Moisselin, J.-M., Walther, G.-R., & Dupouey, J.-L. (2013). Shifts of forest species along an elevational gradient in Southeast France: Climate change or stand maturation? *Journal of Vegetation Science*, *24*(2), 269–283. https://doi.org/10.1111/j.1654-1103.2012.01456.x

Bonan, G. B. (2008). Forests and Climate Change: Forcings, Feedbacks, and the Climate Benefits of Forests. *Science*, *320*(5882), 1444–1449. https://doi.org/10.1126/science.1155121

Carpenter, W., & Goodenough, A. (2014). How robust are community-based plant bioindicators? Empirical testing of the relationship between Ellenberg values and direct environmental measures in woodland communities. *Community Ecology*, *15*(1), 1–11. https://doi.org/10.1556/comec.15.2014.1.1

Chen, J., Saunders, S. C., Crow, T. R., Naiman, R. J., Brosofske, K. D., Mroz, G. D., Brookshire, B. L., & Franklin, J. F. (1999). Microclimate in Forest Ecosystem and Landscape Ecology: Variations in local climate can be used to monitor and compare the effects of different management regimes. *BioScience*, *49*(4). https://doi.org/10.2307/1313612

Christiansen, D. M., Iversen, L. L., Ehrlén, J., & Hylander, K. (2021). Changes in forest structure drive temperature preferences of boreal understorey plant communities. *Journal of Ecology*, *n/a*(n/a). https://doi.org/10.1111/1365-2745.13825

Corlett, R. T., & Westcott, D. A. (2013). Will plant movements keep up with climate change? *Trends in Ecology & Evolution*, *28*(8), 482–488. https://doi.org/10.1016/j.tree.2013.04.003

De Frenne, P., Lenoir, J., Luoto, M., Scheffers, B. R., Zellweger, F., Aalto, J., Ashcroft, M. B., Christiansen, D. M., Decocq, G., De Pauw, K., Govaert, S., Greiser, C., Gril, E., Hampe, A., Jucker, T., Klinges, D. H., Koelemeijer, I. A., Lembrechts, J. J., Marrec, R., … Hylander, K. (2021). Forest microclimates and climate change: Importance, drivers and future research agenda. *Global Change Biology*. https://doi.org/10.1111/gcb.15569

De Frenne, P., Rodriguez-Sanchez, F., Coomes, D. A., Baeten, L., Verstraeten, G., Vellend, M., Bernhardt-Romermann, M., Brown, C. D., Brunet, J., Cornelis, J., Decocq, G. M., Dierschke, H., Eriksson, O., Gilliam, F. S., Hedl, R., Heinken, T., Hermy, M., Hommel, P., Jenkins, M. A., … Verheyen, K. (2013). Microclimate moderates plant responses to macroclimate warming. *Proceedings of the National Academy of Sciences*, *110*(46), 18561–18565. https://doi.org/10.1073/pnas.1311190110

De Frenne, P., Zellweger, F., Rodríguez-Sánchez, F., Scheffers, B. R., Hylander, K., Luoto, M., Vellend, M., Verheyen, K., & Lenoir, J. (2019). Global buffering of temperatures under forest canopies. *Nature Ecology & Evolution*, *3*(5), 744–749. https://doi.org/10.1038/s41559-019-0842-1

De Lombaerde, E., Vangansbeke, P., Lenoir, J., Van Meerbeek, K., Lembrechts, J., Rodríguez-Sánchez, F., Luoto, M., Scheffers, B., Haesen, S., Aalto, J., Christiansen, D. M., De Pauw, K., Depauw, L., Govaert, S., Greiser, C., Hampe, A., Hylander, K., Klinges, D., Koelemeijer, I., … De Frenne, P. (2021). Maintaining forest cover to enhance temperature buffering under future climate change. *Science of The Total Environment*, 151338. https://doi.org/10.1016/j.scitotenv.2021.151338

Dietz, L., Collet, C., Dupouey, J.-L., Lacombe, E., Laurent, L., & Gégout, J.-C. (2020). Windstorm-induced canopy openings accelerate temperate forest adaptation to global warming. *Global Ecology and Biogeography*. https://doi.org/10.1111/geb.13177

Doelman, J. C., Stehfest, E., Tabeau, A., Meijl, H. van, Lassaletta, L., Gernaat, D. E. H. J., Neumann-Hermans, K., Harmsen, M., Daioglou, V., Biemans, H., Sluis, S. van der, & Vuuren, D. P. van. (2018). Exploring SSP land-use dynamics using the IMAGE model: Regional and gridded scenarios of land-use change and land-based climate change mitigation. *Global Environmental Change*, *48*, 119–135. https://doi.org/10.1016/j.gloenvcha.2017.11.014

Dowle, M., & Srinivasan, A. (2020). *data.table: Extension of `data.frame`*. https://CRAN.R-project.org/package=data.table

Dunnington, D., & Thorne, B. (2020). ggspatial: Spatial Data Framework for ggplot2. *R Package Version1*, *1*.

Dupouey, J.-L., Sciama, D., Dambrine, E., Rameau, J.-C., & Koerner, W. (2002). La Végétation des forêts anciennes. *Revue Forestière Française*, *6*, 521. https://doi.org/10.4267/2042/4940

Ellenberg, H., Weber, H.-E., Düll, R., Wirth, V., Werner, W., & Paulißen, D. (1992). *Zeigerwerte von Pflanzen in Mitteleuropa* (Vol. 18).

Ellis, E. C. (2021). Land Use and Ecological Change: A 12,000-Year History. *Annual Review of Environment and Resources*, *46*(1), 1–33. https://doi.org/10.1146/annurev-environ-012220-010822

Euro + Med. (2006). *Euro+Med PlantBase—The information resource for Euro-Mediterranean plant diversity. Http:// www.emplantbase.org/home.html*.

Ewald, J. (2003). The calcareous riddle: Why are there so many calciphilous species in the Central European flora? *Folia Geobotanica*, *38*(4), 357–366. https://doi.org/10.1007/BF02803244

Fick, S. E., & Hijmans, R. J. (2017). WorldClim 2: New 1-km spatial resolution climate surfaces for global land areas. *International Journal of Climatology*, *37*(12), 4302–4315. https://doi.org/10.1002/joc.5086

Franklin, J., Serra-Diaz, J. M., Syphard, A. D., & Regan, H. M. (2016). Global change and terrestrial plant community dynamics. *Proceedings of the National Academy of Sciences*, *113*(14), 3725–3734. https://doi.org/10.1073/pnas.1519911113

Frey, S. J. K., Hadley, A. S., Johnson, S. L., Schulze, M., Jones, J. A., & Betts, M. G. (2016). Spatial models reveal the microclimatic buffering capacity of old-growth forests. *Science Advances*, *2*(4), e1501392. https://doi.org/10.1126/sciadv.1501392

Gégout, J.-C., Coudun, C., Bailly, G., & Jabiol, B. (2005). EcoPlant: A forest site database linking floristic data with soil and climate variables. *Journal of Vegetation Science*, *16*(2), 257–260. https://doi.org/10.1111/j.1654-1103.2005.tb02363.x

Gilliam, F. S. (2007). The Ecological Significance of the Herbaceous Layer in Temperate Forest Ecosystems. *BioScience*, *57*(10), 845–858. https://doi.org/10.1641/B571007

Godefroid, S., Rucquoij, S., & Koedam, N. (2006). Spatial variability of summer microclimates and plant species response along transects within clearcuts in a beech forest. *Plant Ecology*, *185*(1), 107–121. https://doi.org/10.1007/s11258-005-9088-x

Hesslerová, P., Pokorný, J., Brom, J., & Rejšková – Procházková, A. (2013). Daily dynamics of radiation surface temperature of different land cover types in a temperate cultural landscape: Consequences for the local climate. *Ecological Engineering*, *54*, 145–154. https://doi.org/10.1016/j.ecoleng.2013.01.036

Hijmans, R. J. (2020). *raster: Geographic Data Analysis and Modeling*. https://CRAN.R-project.org/package=raster

Hylander, K., Greiser, C., Christiansen, D. M., & Koelemeijer, I. A. (2022). Climate adaptation of biodiversity conservation in managed forest landscapes. *Conservation Biology*, *36*(3), e13847. https://doi.org/10.1111/cobi.13847

IGN. (2019). *BD Forêt version 2*. Institut National de l'Information Géographique et Forestière. https://inventaire-forestier.ign.fr/spip.php?article646

Institute for Environment and Sustainability, Caudullo, G., San Miguel, J., Estreguil, C., & Rigo, D. de. (2013). *Forest landscape in Europe: Pattern, fragmentation and connectivity*. Publications Office of the European Union. https://data.europa.eu/doi/10.2788/77842

Kuhn, E., & Gégout, J. (2019). Highlighting declines of cold-demanding plant species in lowlands under climate warming. *Ecography*, *42*(1), 36–44. https://doi.org/10.1111/ecog.03469

Landuyt, D., De Lombaerde, E., Perring, M. P., Hertzog, L. R., Ampoorter, E., Maes, S. L., De Frenne, P., Ma, S., Proesmans, W., Blondeel, H., Sercu, B. K., Wang, B., Wasof, S., & Verheyen, K. (2019). The functional role of temperate forest understorey vegetation in a changing world. *Global Change Biology*, *25*(11), 3625–3641. https://doi.org/10.1111/gcb.14756

Li, Y., Zhao, M., Motesharrei, S., Mu, Q., Kalnay, E., & Li, S. (2015). Local cooling and warming effects of forests based on satellite observations. *Nature Communications*, *6*(1), Article 1. https://doi.org/10.1038/ncomms7603

Maclean, I. M. D., Hopkins, J. J., Bennie, J., Lawson, C. R., & Wilson, R. J. (2015). Microclimates buffer the responses of plant communities to climate change. *Global Ecology and Biogeography*, *24*(11), 1340–1350. https://doi.org/10.1111/geb.12359

Marrec, R., Gril, E., Spicher, F., Vital, G., & Lenoir, J. (2022). *Can flora predict forest microclimate?* https://doi.org/10.13140/RG.2.2.29973.40165

Martin, G., Devictor, V., Motard, E., Machon, N., & Porcher, E. (2019). Short-term climate-induced change in French plant communities. *Biology Letters*, *15*(7), 20190280. https://doi.org/10.1098/rsbl.2019.0280

Meeussen, C., Govaert, S., Vanneste, T., Bollmann, K., Brunet, J., Calders, K., Cousins, S. A. O., De Pauw, K., Diekmann, M., Gasperini, C., Hedwall, P.-O., Hylander, K., Iacopetti, G., Lenoir, J., Lindmo, S., Orczewska, A., Ponette, Q., Plue, J., Sanczuk, P., … De Frenne, P. (2021). Microclimatic edge-to-interior gradients of European deciduous forests. *Agricultural and Forest Meteorology*. https://doi.org/10.1016/j.agrformet.2021.108699

Osman, K. T. (2013). Forest Soils. In K. T. Osman (Ed.), *Soils: Principles, Properties and Management* (pp. 229–251). Springer Netherlands. https://doi.org/10.1007/978-94-007-5663-2_14

Pebesma, E. (2018). Simple Features for R: Standardized Support for Spatial Vector Data. *The R Journal*, *10*(1), 439–446. https://doi.org/10.32614/RJ-2018-009

Pecl, G. T., Araújo, M. B., Bell, J. D., Blanchard, J., Bonebrake, T. C., Chen, I.-C., Clark, T. D., Colwell, R. K., Danielsen, F., Evengård, B., Falconi, L., Ferrier, S., Frusher, S., Garcia, R. A., Griffis, R. B., Hobday, A. J., Janion-Scheepers, C., Jarzyna, M. A., Jennings, S., … Williams, S. E. (2017). Biodiversity redistribution under climate change: Impacts on ecosystems and human well-being. *Science*. https://doi.org/10.1126/science.aai9214

Piedallu, C., Chéret, V., Denux, J. P., Perez, V., Azcona, J. S., Seynave, I., & Gégout, J. C. (2019). Soil and climate differently impact NDVI patterns according to the season and the stand type. *Science of The Total Environment*, *651*, 2874–2885. https://doi.org/10.1016/j.scitotenv.2018.10.052

Pokorny, J., Brom, J., Cermak, J., Hesslerova, P., Huryna, H., Nadezhdina, N., & Rejskova, A. (2010). Solar energy dissipation and temperature control by water and plants. *International Journal of Water*, *5*(4), 311–336. https://doi.org/10.1504/IJW.2010.038726

Prevedello, J. A., Winck, G. R., Weber, M. M., Nichols, E., & Sinervo, B. (2019). Impacts of forestation and deforestation on local temperature across the globe. *PLOS ONE*, *14*(3), e0213368. https://doi.org/10.1371/journal.pone.0213368

R Core Team. (2019). *R: A Language and Environment for Statistical Computing*. R Foundation for Statistical Computing. https://www.R-project.org/

Richard, B., Dupouey, J.-L., Corcket, E., Alard, D., Archaux, F., Aubert, M., Boulanger, V., Gillet, F., Langlois, E., Macé, S., Montpied, P., Beaufils, T., Begeot, C., Behr, P., Boissier, J.-M., Camaret, S., Chevalier, R., Decocq, G., Dumas, Y., … Lenoir, J. (2021). The climatic debt is growing in the understorey of temperate forests: Stand characteristics matter. *Global Ecology and Biogeography*, *n/a*(n/a). https://doi.org/10.1111/geb.13312

Sanczuk, P., De Lombaerde, E., Haesen, S., Van Meerbeek, K., Luoto, M., Van der Veken, B., Van Beek, E., Hermy, M., Verheyen, K., Vangansbeke, P., & De Frenne, P. (2022). Competition mediates understorey species range shifts under climate change. *Journal of Ecology*, *110*(8), 1813–1825. https://doi.org/10.1111/1365-2745.13907

Saura, S., Martín-Queller, E., & Hunter, M. L. (2014). Forest landscape change and biodiversity conservation. In J. C. Azevedo, A. H. Perera, & M. A. Pinto (Eds.), *Forest Landscapes and Global Change: Challenges for Research and Management* (pp. 167–198). Springer. https://doi.org/10.1007/978-1-4939-0953-7_7

Stanturf, J. A., Palik, B. J., & Dumroese, R. K. (2014). Contemporary forest restoration: A review emphasizing function. *Forest Ecology and Management*, *331*, 292–323. https://doi.org/10.1016/j.foreco.2014.07.029

Stark, J. R., & Fridley, J. D. (2022). Microclimate-based species distribution models in complex forested terrain indicate widespread cryptic refugia under climate change. *Global Ecology and Biogeography*, *31*(3), 562–575. https://doi.org/10.1111/geb.13447

Szymura, T. H., Szymura, M., & Macioł, A. (2014). Bioindication with Ellenberg's indicator values: A comparison with measured parameters in Central European oak forests. *Ecological Indicators*, *46*, 495–503. https://doi.org/10.1016/j.ecolind.2014.07.013

Thomas, C. D., Cameron, A., Green, R. E., Bakkenes, M., Beaumont, L. J., Collingham, Y. C., Erasmus, B. F. N., de Siqueira, M. F., Grainger, A., Hannah, L., Hughes, L.,

Huntley, B., van Jaarsveld, A. S., Midgley, G. F., Miles, L., Ortega-Huerta, M. A., Townsend Peterson, A., Phillips, O. L., & Williams, S. E. (2004). Extinction risk from climate change. *Nature*, *427*(6970), 145–148. https://doi.org/10.1038/nature02121

Valdés, A., Lenoir, J., De Frenne, P., Andrieu, E., Brunet, J., Chabrerie, O., Cousins, S. A. O., Deconchat, M., De Smedt, P., Diekmann, M., Ehrmann, S., Gallet-Moron, E., Gärtner, S., Giffard, B., Hansen, K., Hermy, M., Kolb, A., Le Roux, V., Liira, J., … Decocq, G. (2020). High ecosystem service delivery potential of small woodlands in agricultural landscapes. *Journal of Applied Ecology*, *57*(1), 4–16. https://doi.org/10.1111/1365-2664.13537

Vallauri, D., Grel, A., Granier, E., & Dupouey, J.-L. (2012). *Les forêts de Cassini. Analyse quantitative et comparaison avec les forêts actuelles* (p. 65 p.) [Technical Report]. WWF. https://hal.archives-ouvertes.fr/hal-01267936

Vangansbeke, P., Máliš, F., Hédl, R., Chudomelová, M., Vild, O., Wulf, M., Jahn, U., Welk, E., Rodríguez-Sánchez, F., & Frenne, P. D. (2021). ClimPlant: Realized climatic niches of vascular plants in European forest understoreys. *Global Ecology and Biogeography*, *30*(6), 1183–1190. https://doi.org/10.1111/geb.13303

Vanneste, T., Govaert, S., Spicher, F., Brunet, J., Cousins, S. A. O., Decocq, G., Diekmann, M., Graae, B. J., Hedwall, P.-O., Kapás, R. E., Lenoir, J., Liira, J., Lindmo, S., Litza, K., Naaf, T., Orczewska, A., Plue, J., Wulf, M., Verheyen, K., & De Frenne, P. (2020). Contrasting microclimates among hedgerows and woodlands across temperate Europe. *Agricultural and Forest Meteorology*, *281*, 107818. https://doi.org/10.1016/j.agrformet.2019.107818

Wickham, H. (2011). Ggplot2. *WIREs Computational Statistics*, *3*(2), 180–185. https://doi.org/10.1002/wics.147

Zellweger, F., De Frenne, P., Lenoir, J., Vangansbeke, P., Verheyen, K., Bernhardt-Römermann, M., Baeten, L., Hédl, R., Berki, I., Brunet, J., Van Calster, H., Chudomelová, M., Decocq, G., Dirnböck, T., Durak, T., Heinken, T., Jaroszewicz, B., Kopecký, M., Máliš, F., … Coomes, D. (2020). Forest microclimate dynamics drive plant responses to warming. *Science*, *368*(6492), 772–775. https://doi.org/10.1126/science.aba6880

Zuur, A. F., Ieno, E. N., & Elphick, C. S. (2010). A protocol for data exploration to avoid common statistical problems. *Methods in Ecology and Evolution*, *1*(1), 3–14. https://doi.org/10.1111/j.2041-210X.2009.00001.x

6. Data Availability

French National Forest Inventory data are freely available through the Institute for Geographic and Forest Information (IGN) at https://inventaire-forestier.ign.fr/ .
All the data used in this study as well as the code to run and reproduce the analyses can be downloaded and cloned from GitHub: https://github.com/Jeremy-borderieux/Article_Landscape_Forest_Cool_Comm.git

aknowledgment

7. Acknowledgments

The authors are grateful to the French institute for geographic and forest information (IGN) for providing the NFI data and the French forest cover map (BD forêt V2). The authors thank Jean-Daniel Bontemps and Jonathan Lenoir for their fruitful comments. JB was funded by a joint AgroParisTech and Région Grand-Est grant (grant number 19_GE8_01020p05035) and JMSD was funded by the ANR-JCJC SEEDFOR (ANR-21-CE32-0003). JMSD acknowledges the support from from NASA for UConn's Ecological Modeling Institute (#80NSSC 22K0883). The authors are thankful to Vicki Moore for reviewing the language.

8. Supplementary materials

Supplementary Table 1: Coefficients (Estimate), Standard errors, P-values, and effect size of the parameter of the canopy cover model fitted with 1,940 pairs. Effect sizes were computed by multiplying an estimate by the mean pairwise differences of the corresponding parameter (except for the intercept).

Parameter	Estimate	Std. Error	P-value	Effect size
Intercept	-0.131	0.024	$<10^{-4}$	-0.13
Δ Elevation	0.00293	0.00083	$<10^{-4}$	0.028
Δ Mean annual temperature	0.281	0.087	0.0013	-0.016
Δ Ellenberg L	-0.173	0.022	$<10^{-4}$	0.0069
Δ Bioindicated pH	0.316	0.026	$<10^{-4}$	-0.24
Δ Ellenberg N	-0.117	0.021	$<10^{-4}$	0.094
Δ Year	0.00555	0.0031	0.077	-0.008
Δ Canopy cover	0.00136	0.00063	0.032	0.00083

Supplementary Table 2: Coefficients (Estimate), Standard errors, P-values, and effect size of the parameter of the distance to the edge model fitted with 309 pairs. Effect sizes were computed by multiplying an estimate by the mean pairwise differences of the corresponding parameter (except for the intercept).

Parameter	Estimate	Std. Error	P-value	Effect size
Intercept	-0.186	0.083	0.026	-0.19
Δ Elevation	0.00251	0.0019	0.2	0.026
Δ MAT	0.175	0.19	0.36	-0.0063
Δ Ellenberg L	-0.219	0.049	$<10^{-4}$	-0.0053
Δ Bioindicated pH	0.342	0.065	$<10^{-4}$	-0.29
Δ Ellenberg N	-0.192	0.052	$<10^{-4}$	0.18
Δ Year	0.0133	0.02	0.51	-0.0032
Δ Distance to the edge	-0.000143	0.00017	0.41	-0.046

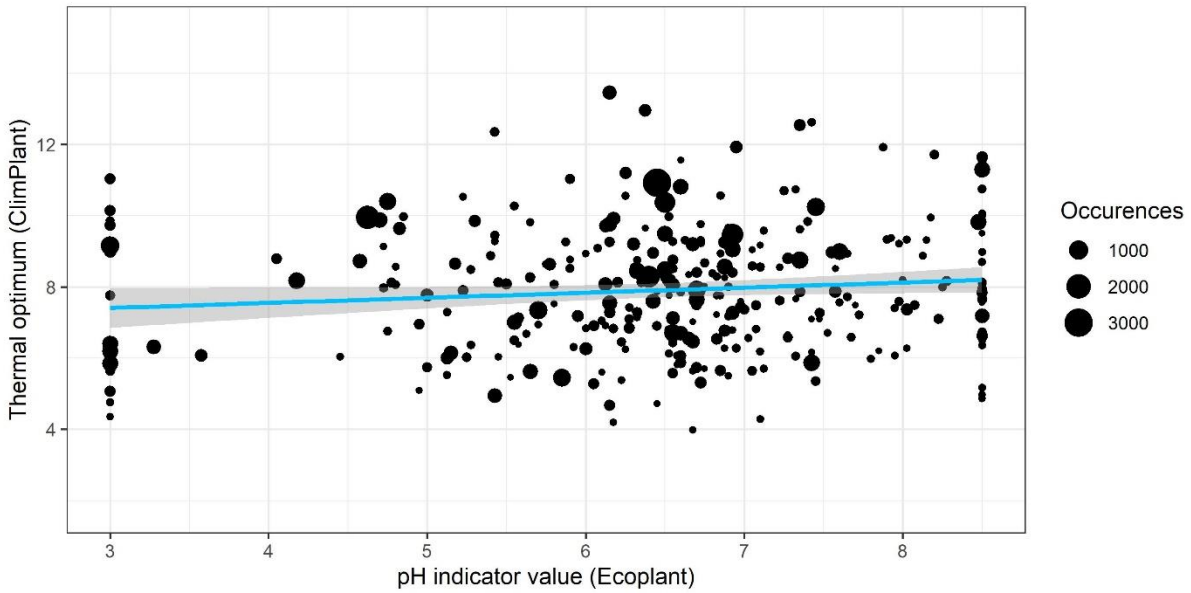

Supplementary Figure 1: Thermal optimum of a species as a function of its pH indicator value. The occurrence of a species in the dataset (n= 4,024) is represented by the size. The blue line represents a fitted linear model and its error. (coefficient= 0.142, P-value=0.0613).

Supplementary Table 3: Coefficients (Estimate), Standard errors, P-values of the linear model $Thermal\ optimum \sim pH_{indicator\ value} + N\ Ellenberg$ *. The model was fitted with 243 species recorded in the dataset of 4,024 plots.*

Parameters	Estimate	Std. Error	P-value
Intercept	7.11	0.594	$<10^{-4}$
pH indicator value	0.161	0.0826	0.0527
N Ellenberg	-0.0460	0.0543	0.398